SUPPORTING INFORMATION

Introduction to lens structure

Lens epithelium and fibers. In the anterior lens, the epithelial cell monolayer regulates the transport and permeability of water, electrolytes and other compounds between aqueous humor and the lens[1]. Lens epithelial cells possess tight and adherens junctions and active transport for electrolytes and amino acids. During lens growth and aging, anterior to lens equator, the epithelial cells undergo mitosis and migrate to the lens equator, and then differentiate and elongate into lens fiber cells, which do not have nuclei or other organelles. The lens fiber cells lay over the older cells, forming a core-like structure. The lens fibers can be further divided into lens cortex and nucleus: the cortex comprises of the youngest lens fibers and is loose and soft in consistency, whereas the lens nucleus contains the oldest lens fibers in a compact arrangement, resulting in a dense consistency.

The lens capsule. Epithelial and fiber cells are completely enveloped by the lens capsule, the thickest basement membrane in the body, which has various roles in lens mechanics and cell survival[2]. Moreover, the lens is suspended by the capsule and the collagenous zonule fibers from the ciliary muscles. The lens capsule, produced by the lens epithelial cells and the fiber cells, is a lamellar structure consisting of laminin, type IV collagen, entactin/nidogen and proteoglycans[2]. The capsule is the thickest just anterior and posterior to lens the equator, in the regions where zonules attach to it, and thins towards the anterior and posterior poles[1]. In the pole areas, the capsule thickness is 5-10 fold greater in the anterior than posterior side. As an example, in adult human the capsule thickness ranges from 4 μm (posterior pole) to 23 μm (near equator).

Lens composition. The lens composes mostly of water (65% of wet weight) and protein (34% of wet weight), most of which are various crystallins, and 1% of other compounds, such as lipids, inorganic ions, glucose, ascorbic acid and amino acids. The water, protein and lipid content in the lens varies between the cortex and nucleus. The cortex, consisting of the younger, softer fiber cells, has higher water content and lower protein and lipid contents than the nucleus. In contrast, the lens nucleus with the tightly-packed fiber cells contains more protein and protein-bound lipids and less water than the cortex.

For in-depth review on lens growth and structure of the lens, see [3], and capsule structure, see [2].

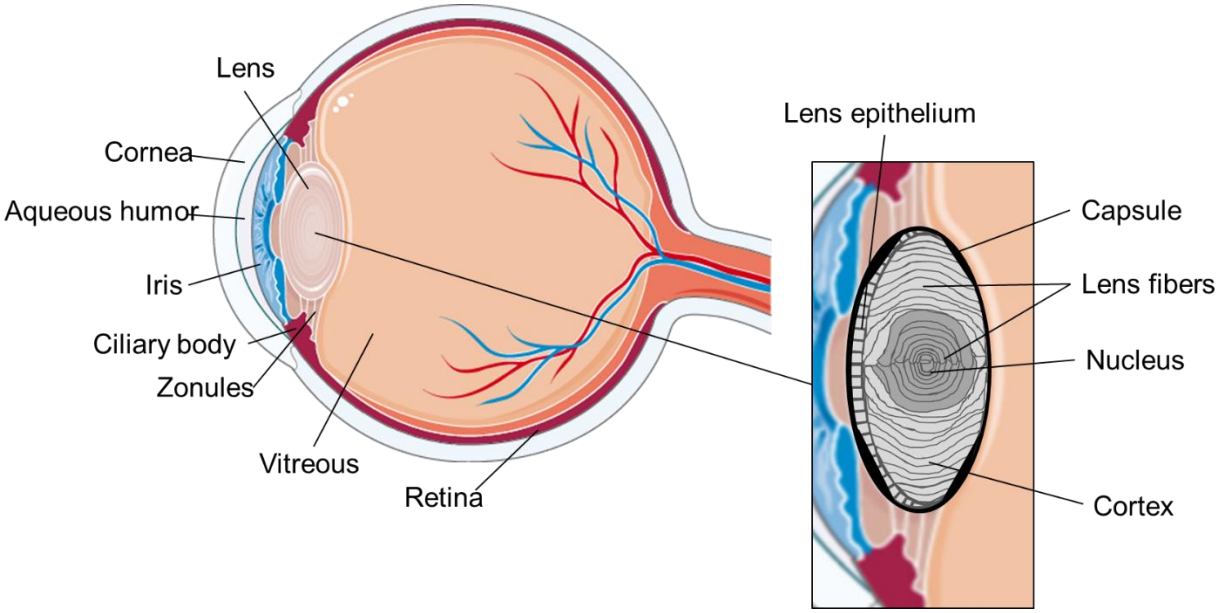

Supplementary figure 1. Location of the lens in the eye and its structure. The main substructures of the lens are the lens epithelium, fiber cells and the capsule. Lens fiber cells can be further divided into the lens cortex, comprising of the youngest fiber cells, and to lens nucleus, containing the oldest. (adapted from Servier Medical Art by Servier, licensed under a Creative Commons Attribution 3.0 Unported License)

Lens mass during incubation

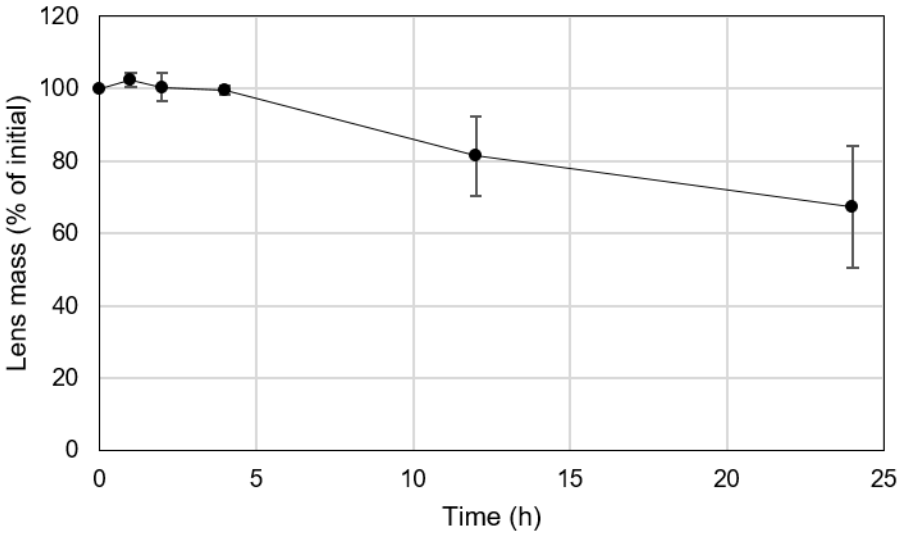

Supplementary figure 2. Lens mass during incubation in HBSS-Hepes (pH 7.4) at +37º C with 150 rpm shaking (mean ± SD, n = 2, except at 0 and 24 h n=10).

MALDI IMS: standard solution loading on a blank lens

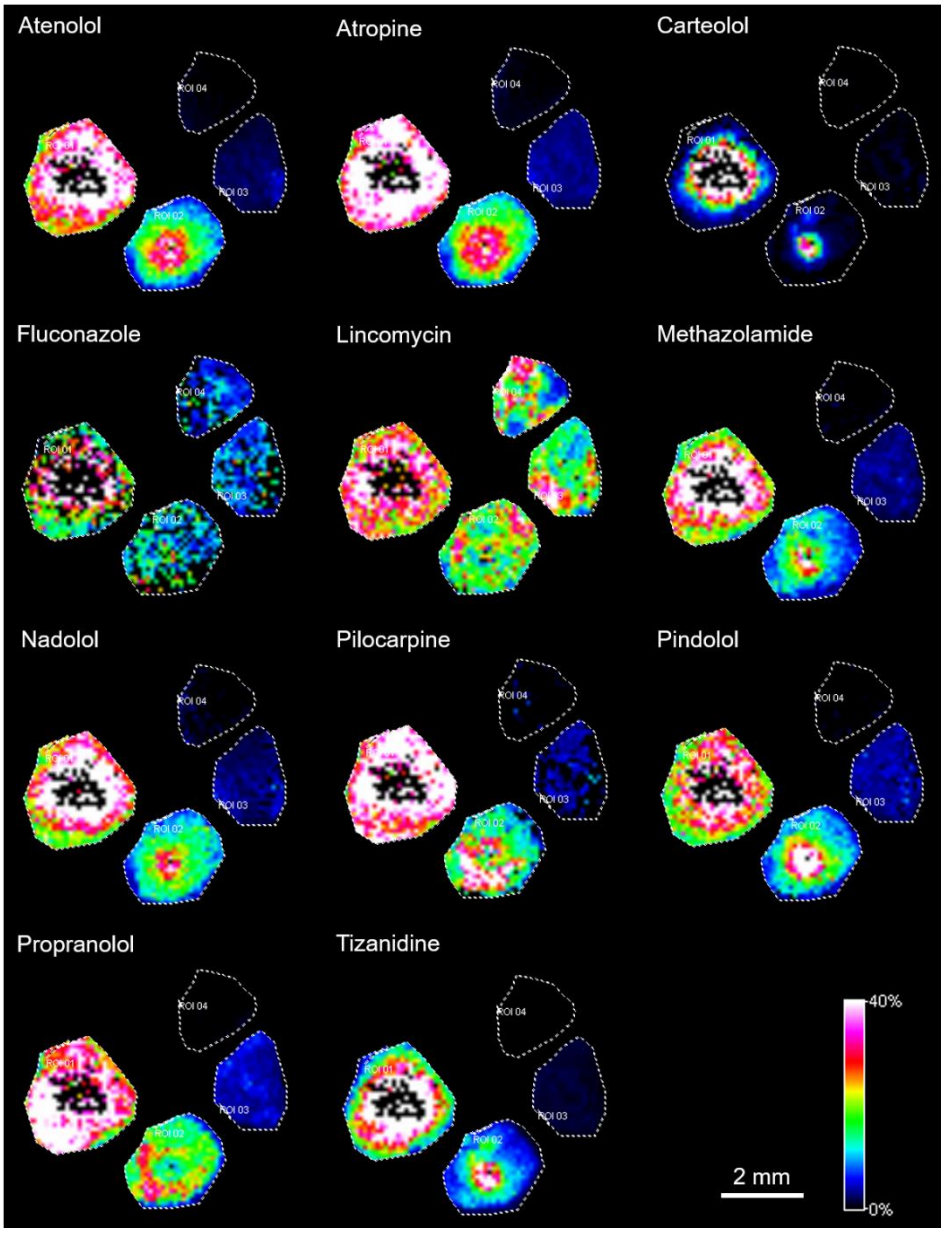

Supplementary figure 3. Standard solution loading on a blank lens in MALDI IMS. The pipetted drug amounts were 0.1, 0.5, 2 and 10 ng.

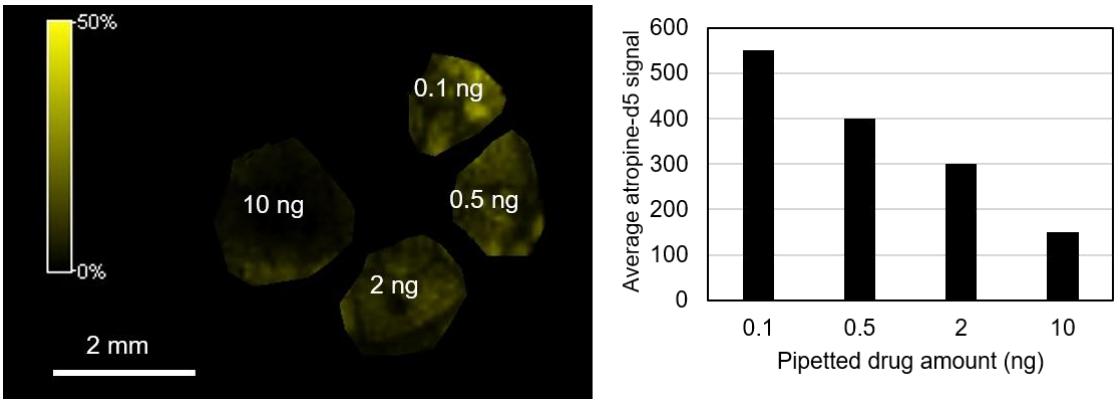

Supplementary figure 4. Internal standard atropine-d5 signal in blank lenses loaded with cassette mix drug standards (0.1, 0.5, 2 and 10 ng). Atropine-d5 signal is suppressed, when the loaded drug amount in the lens increases.

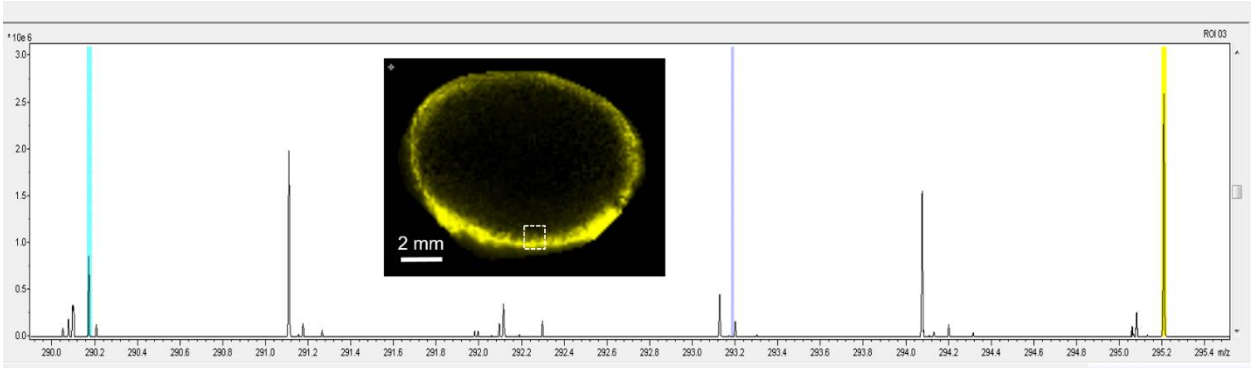

Supplementary figure 5. Average IMS spectrum of the posterior lens surface (1mm thickness) showing atropine at m/z 290.176 (turquoise) and D-5 atropine at m/z 295.206 (yellow).

Calculating the apparent volume of distribution in the lens

In addition to the anatomical volume of the lens, the K_p values were also calculated using the estimated true distribution volume in the surface layer of the lens. Based on the MALDI-IMS images of drug distribution in lens section for atropine, pindolol, propranolol, pilocarpine and tizanidine, it seems that despite the five drugs display different log$D_{7.4}$ values, they had roughly the same spatial distribution: most of the lens section does not contain drugs, and the drugs distribute only to a small volume in the outer lens. This assumption was extended also to the other compounds. In the calculations, we assumed that the diameter of the lens area clear from the drugs is roughly 90% of the total lens diameter. Thus, the true distribution volume can be calculated by subtracting the unoccupied volume from the total volume. Supplementary equation 1 was reduced to a numerical value of the ratio between the true distribution volume and anatomical lens volume.

$$\frac{V_{true}}{V_{total}} = \frac{V_{total} - V_{clear}}{V_{total}} = \frac{\frac{\pi}{6}A^2B - \frac{\pi}{6}\cdot(0.9A)^2\cdot 0.9B}{\frac{\pi}{6}A^2B} = 0.271 \approx 27\% \quad (1)$$

where A is the equatorial diameter and B is the polar diameter.

Pharmacokinetic simulations

The pharmacokinetic simulation model was built on a model of topical timolol instillation[4], where a lens compartment, separate from the reservoir compartment, was added. Experimental concentration-time data, extracted with Webplotdigitizer (v4.2, https://automeris.io/WebPlotDigitizer), in the aqueous humor and lens after topical dosing of timolol[5] was used as a basis for the lens compartment.

The timolol distribution clearance between aqueous humor and lens (Q_{LENS}), lens-buffer partition coefficient (K_p) and clearance from tear fluid to cornea ($CL_{TF,CO}$) were obtained by comparing the simulated curves with experimental in vivo data on timolol distribution in the rabbit lens[5]. The parameter values were adjusted manually until a good fit between the simulated and the observed concentration in the lens was achieved (Supplementary figure 6). Based on the final K_p and Q_{LENS} values, the distribution clearance between aqueous humor and reservoir ($Q_{RESERVOIR}$) and volume of the reservoir ($V_{RESERVOIR}$) were changed to match the corresponding parameters in the original model[4] (Supplementary table 1).

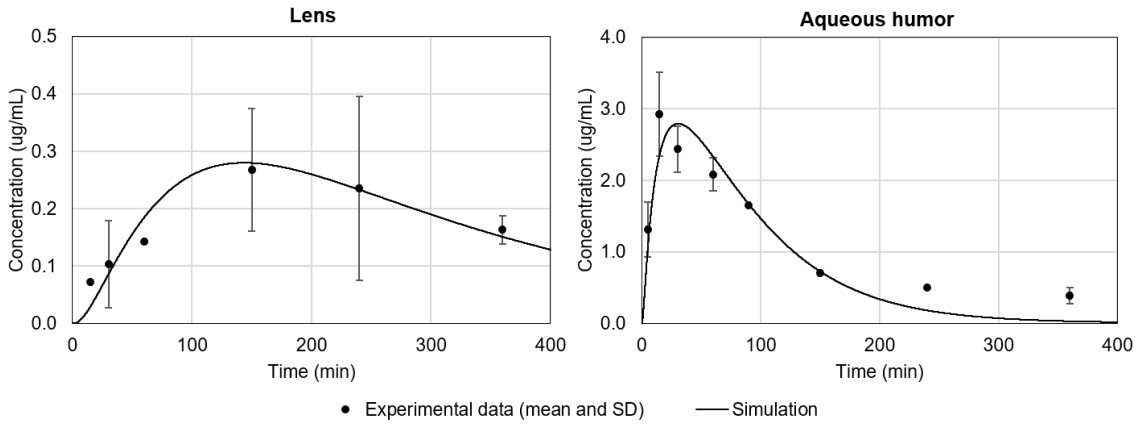

Supplementary figure 6. Adjustment of the lens-aqueous humor partition coefficient (K_p), the clearance between aqueous humor and lens (Q_{LENS}) and clearance from tear fluid to cornea ($CL_{TF,CO}$) with experimental data[5].

Supplementary table 1. Parameters for the pharmacokinetic simulation model.

Parameter	**Value**	**Source**
V_{TF}	$V_{RES} + V_{INS} \exp(-k_{drain}\, t)$	[4]
V_{RES}	7.5 µL	[4,6]
V_{INS}	25 µL	[4]
k_{drain}	0.545 min^{-1}	[4,6]
CL_{drain}	$k_{drain}[V_{INS} \exp(-k_{drain}\, t)]$	[4]
CL_{TT}	0.53 µL min^{-1}	[4,6]
$CL_{TF,CJ}$	10.4 µL min^{-1}	[4,7]
k_D	0.0179 min^{-1}	[4]
k_{el}	0.057 min^{-1}	[4,8]
V_{AQ}	446 µL	[4,8]
V_{LENS}	403 µL	[9,10]
$CL_{TF,CO}$	1.3 µL min^{-1}	Adjusted with experimental data[5]
Q_{LENS}	0.6 µL min^{-1}	Adjusted with experimental data[5]
K_p	0.35	Adjusted with experimental data[5]
$V_{RESERVOIR}$	262 µL	Adjusted from from original model[4] *
$Q_{RESERVOIR}$	11.888 µL min^{-1}	Adjusted from from original model[4] **

* $V_{RESERVOIR} = V2 - V_{app,lens} = \frac{k12 \cdot V1}{k21} - V_{LENS} \cdot K_p = \frac{0.028\, min^{-1} \cdot 446\, \mu L}{0.031\, min^{-1}} - 406\, \mu L \cdot 0.35$; parameter values for V1, V2, k_{12} and k_{21} from Ranta et al. [4]

** $Q_{RESERVOIR} = k12 \cdot V2 - Q_{LENS} = 0.028\, min^{-1} \cdot \frac{k12 \cdot V1}{k21} - 0.6\, \mu L\, min^{-1}$; parameter values for V1, V2, k_{12} and k_{21} from Ranta et al. [4]

Drug concentration equilibrium in the in vitro system

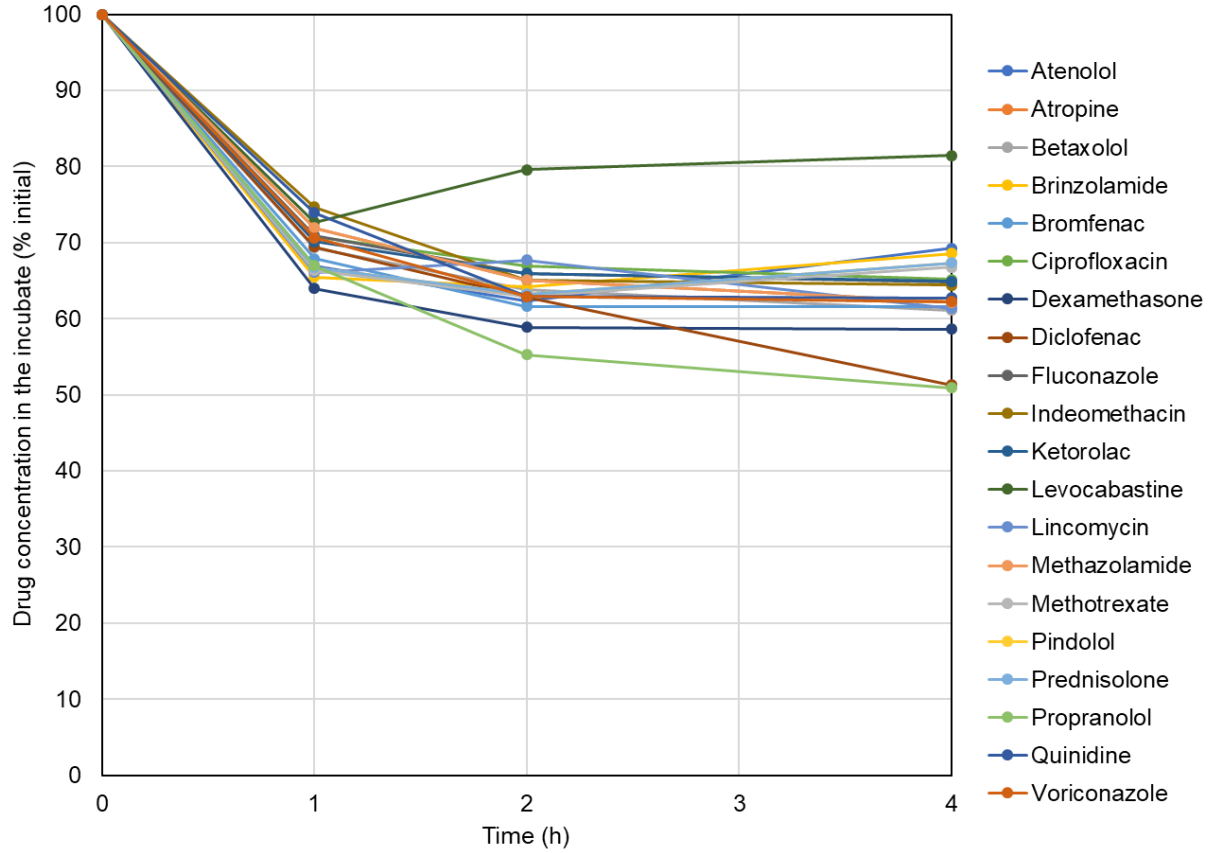

Supplementary figure 7. Drug concentration in the incubate as % initial for 20 compounds (mean, n=4, standard deviation not shown for clarity). The drugs were incubated in vitro with isolated porcine lenses.

Literature

1. Dai E, Boulton ME. Basic science of the lens. In: Yanoff M, Diker J, eds. *Ophtalmology.* Edinburgh: Elsevier; 2018:381-393.
2. Danysh BP, Patel TP, Czymmek KJ, et al. Characterizing molecular diffusion in the lens capsule. *Matrix Biology*. 2010;29(3):228-236.
3. Augusteyn RC. On the growth and internal structure of the human lens. *Experimental Eye Research*. 2010;90(6):643-654.
4. Ranta V, Laavola M, Toropainen E, Vellonen K, Talvitie A, Urtti A. Ocular pharmacokinetic modeling using corneal absorption and desorption rates from in vitro permeation experiments with cultured corneal epithelial cells. *Pharm Res*. 2003;20(9):1409-1416.
5. Lee VH, Luo AM, Li SY, et al. Pharmacokinetic basis for nonadditivity of intraocular pressure lowering in timolol combinations. *Investigative Ophthalmology & Visual Science*. 1991;32(11):2948.
6. Chrai SS, Patton TF, Mehta A, Robinson JR. Lacrimal and instilled fluid dynamics in rabbit eyes. *Journal of Pharmaceutical Sciences*. 1973;62(7):1112-1121.
7. Ahmed I, Patton TF. Disposition of timolol and inulin in the rabbit eye following corneal versus non-corneal absorption. *International Journal of Pharmaceutics*. 1987;38(1):9-21.
8. Yamamura K, Sasaki H, Nakashima M, et al. Characterization of ocular pharmacokinetics of beta-blockers using a diffusion model after instillation. *Pharm Res*. 1999;16(10):1596-1601.
9. Struble C, Howard S, Relph J. Comparison of ocular tissue weights (volumes) and tissue collection techniques in commonly used preclinical animal species. *Acta Ophthalmologica*. 2014;92(s253):0.
10. Vilupuru AS, Glasser A. Optical and biometric relationships of the isolated pig crystalline lens. *Ophthalmic and Physiological Optics*. 2001;21(4):296-311.